mining

MDPI

Article

Particle-Level Changes in Respirable Coal Mine Dust Characteristics, 2003–2020

Emily Sarver *, Çigdem Keleş, Setareh Ghaychi Afrouz and Eleftheria Agioutanti

Department of Mining and Minerals Engineering, Virginia Polytechnic Institute and State University, Blacksburg, VA 24060, USA

* Correspondence: esarver@vt.edu

Abstract

Mining practices and operating conditions are continually evolving, and the respirable fraction of coal mine dust is accordingly expected to change in composition and particle characteristics over time. Between the early 2000s and late 2010s, several regulatory and operational changes occurred in U.S. underground coal mining that could plausibly influence respirable coal mine dust (RCMD), including expanded rock-dusting practices, increased emphasis on respirable crystalline silica, and reductions in diesel emissions. This study evaluated temporal differences in RCMD by comparing samples collected in 2003–2005 and 2018–2020 using particle-level scanning electron microscopy with energy-dispersive X-ray spectroscopy (SEM–EDX). The most consistent temporal change observed was an increase in carbonate particles, consistent with expanded rock-dusting practices. Shifts in coal- and rock-strata-derived dust were observed but were not consistent across regions, and no consistent trend toward finer particle sizes was identified. These results demonstrate the value of particle-level analysis for evaluating changes in RCMD characteristics over time.

Keywords: respirable coal mine dust; black lung; pneumoconiosis; dust characterization; SEM-EDX; thin seam mining; rock dusting

1. Introduction

Much of what is known about respirable coal mine dust (RCMD) exposure in U.S. mines has been derived from sampling conducted to demonstrate regulatory compliance [1,2]. These monitoring efforts have conventionally yielded two primary metrics: the time-weighted average mass concentration of respirable dust and the crystalline silica content within that dust (reported as mass percentage, from which the mass concentration can also be derived). Over the past several decades, both metrics have generally trended downward [1,3,4]. While these mass-based indicators remain central to exposure assessment and regulation, they do not fully describe the physical and chemical characteristics of RCMD that may influence toxicity [2]. Respirable dust in coal mines is a heterogeneous mixture of particles derived from coal seams, surrounding rock strata, and engineered materials introduced into the mine environment, and differences in particle size distributions and mineralogical composition may have important implications for health risk [2].

Interest in RCMD characteristics beyond mass concentration has been heightened by the resurgence of severe and rapidly progressive lung disease among U.S. coal miners since the late 1990s, particularly in central Appalachia [5–11]. This trend appears incongruent with long-term declines in measured respirable dust and quartz concentrations, leading to speculation that changes in mining practices and technologies may have altered the

Check for updates

Academic Editor: Vasyl Lozynskyi

Received: 6 March 2026
Revised: 5 April 2026
Accepted: 9 April 2026
Published: 13 April 2026

Copyright: © 2026 by the authors. Licensee MDPI, Basel, Switzerland. This article is an open access article distributed under the terms and conditions of the Creative Commons Attribution (CC BY) license.

nature of dust exposures over time [2]. For example, the extraction of increasingly thinner coal seams may necessitate greater cutting of roof and floor rock, potentially increasing the proportion of mineral particles in RCMD, while more powerful cutting equipment or changes in dust-control strategies might have influenced particle size distributions [12–14]. Collectively, these considerations underscore the importance of examining how RCMD characteristics may evolve over time.

Despite strong interest in understanding temporal trends in RCMD characteristics, direct evaluation has been limited by the scarcity of historical dust samples and data suitable for detailed characterization [2]. Samples collected for regulatory purposes are typically not retained after gravimetric analysis—and standard quartz analysis is destructive—and thus are unavailable for retrospective study [2]. Although numerous studies, including multiple works by the authors, have provided detailed characterization of RCMD samples collected from U.S. mines in recent years [12,13], there is little comparable information from earlier periods. This gap was explicitly identified in a 2018 National Academies report, which called for targeted research to better understand how dust characteristics may have changed over time [2].

The early 2000s to late 2010s represent a period during which several major regulatory and operational changes occurred in U.S. underground coal mining that could plausibly influence RCMD characteristics. First, the resurgence of occupational lung disease renewed attention on coal miner health and ultimately led to the Mine Safety and Health Administration's (MSHA) "new dust rule," published in 2014 and fully implemented in 2016 [2]. The rule lowered the permissible exposure limit for RCMD and mandated more frequent monitoring using new technology. While compliance monitoring data indicate that mine operators have generally succeeded in reducing mass-based dust exposures [15], it remains unclear how these reductions may have affected particle size distributions or the relative abundance of specific dust constituents, such as silica (Jaramillo et al., 2022) [13]. For example, specific dust controls such as water sprays, improved ventilation, and modifications to drilling and cutting practices may have had an effect.

Second, explosions at two West Virginia mines—the Sago Mine in 2006 and the Upper Big Branch Mine in 2010—prompted increased requirements for rock dusting [3]. Rock dusting involves the application of fine inert material, typically composed of high-purity limestone or dolostone powder, to mine surfaces [2]. While this practice can mitigate explosibility hazards, it can also contribute to the respirable dust fraction in the mine atmosphere [12,13], and it is unclear how much the situation changed following these events, which prompted greater emphasis on rock-dusting efforts [16]. The extent to which increased rock dusting has altered RCMD composition over time has not been systematically evaluated.

Third, regulatory efforts initiated in the early 2000s to limit diesel particulate matter (DPM) emissions from underground equipment have driven gradual transitions away from older, high-emission engines, potentially reducing the abundance of fine carbonaceous particles in respirable dust [17]; however, the long-term impact on RCMD characteristics remains largely unexamined.

In this context, the objective of the current study was to evaluate whether and how RCMD characteristics have changed over time by directly comparing samples collected during two distinct periods. Earlier samples were obtained through collaboration with the CDC/NIOSH Pittsburgh Mining Research Division and were originally collected between 2003 and 2005, whereas later samples were collected by the authors between 2018 and 2020. In this study, RCMD characteristics are evaluated at the particle level using particle-level scanning electron microscopy with energy-dispersive X-ray spectroscopy (SEM-EDX), which enables simultaneous assessment of particle size and mineralogical

composition [13,18,19]. By examining these characteristics between the two timeframes, this work seeks to provide insight into the magnitude and nature of temporal changes in RCMD during a period of substantial regulatory and operational evolution in U.S. coal mining.

2. Materials and Methods

2.1. Sample Selection

As described above, this study compares RCMD characteristics between samples collected during two distinct timeframes: an earlier period (2003–2005) and a later period (2018–2020). To ensure valid temporal comparisons, it was essential that samples from both timeframes represent comparable dust-generating environments and were collected using identical sampling configurations, consistent with regulatory and research practice for respirable dust monitoring [2,3].

A total of 59 samples were provided by the CDC/NIOSH Pittsburgh Mining Research Division (Table 1). All earlier samples were collected at active mining (AM) locations as part of prior federal research studies. In this context, AM locations refer broadly to areas in close proximity to active coal extraction activities, including cutting at the mine face and roof bolting, and in the ventilation returns just outby the mining activity. These samples were collected on 37 mm polyvinyl chloride (PVC) filters (nominal 5 µm pore size) using standard gravimetric sampling trains consisting of a 10 mm nylon cyclone operated at 2 L min^{-1}, which corresponds to the U.S. respirable dust sampling convention ([2]; MSHA, 2017 [3]). Metadata identifying the sampling year and MSHA district were available for all samples.

Table 1. Summary of RCMD samples analyzed for this project from the earlier and later timeframes. (NA = northern Appalachia, CA = central Appalachia, MW = mid-west, W = west, CKY = central Kentucky, AL = Alabama).

	Region						
Timeframe	CA	NA	MW	W	CKY	AL	Total
Earlier (2003–2005)	11	13	3	10	13	9	59
Later (2018–2020)	13	8	6	3	-	-	30

To enable meaningful temporal comparisons, later samples from the authors' inventory were restricted to locations that reasonably represent comparable dust-generating activities, specifically production (P), roof bolting (B), and return (R) locations, which are known to capture coal-cutting, rock cutting, and mixed-source dust environments [20]. Application of these criteria yielded 30 later samples collected between 2018 and 2020 from underground coal mines in central Appalachia (CA), northern Appalachia (NA), the Midwest (MW), and the West (W). These samples were quantitatively compared with 37 earlier samples from the same four regions, all collected at AM locations.

Notably, while detailed metadata on exact sampling locations were limited for some earlier samples, available documentation and communication with investigators involved in the original studies indicate that AM sampling locations were broadly consistent with the sampling strategy used for the later dataset. Nonetheless, differences in specific sampling locations could contribute to some variability in the observed results. As a result, comparisons between timeframes should be interpreted as reflecting broadly similar dust-generating environments rather than identical sampling locations.

Additional earlier samples from central Kentucky (CKY) (n = 13) and Alabama (AL) (n = 9) were also available (Table 1). Because no later samples were available from these re-

gions, they were excluded from statistical analyses but retained for descriptive comparisons to provide a broader regional context.

2.2. Sample Preparation

Although PVC filters are standard for gravimetric sampling of respirable dust, dust particle characterization by SEM-EDX requires deposition onto a flat, non-fibrous substrate [21]. Particles were therefore recovered from the PVC filters and redeposited onto polycarbonate (PC) filters using a wet-recovery procedure adapted from Greth et al. (2024) [21]. Briefly, each filter (or a representative section) was placed in a clean glass tube, submerged in isopropyl alcohol (IPA), and sonicated for several minutes to release particles from the PVC matrix. The resulting suspension was transferred to a vacuum filtration unit and deposited onto a 47 mm PC filter. For samples with very low dust mass, the suspension was instead pushed through a 25 mm PC filter using a syringe to increase particle density. After drying, a 9 mm subsection was carefully cut from the PC filter and sputter-coated with a thin Au/Pd layer to ensure conductivity during SEM analysis.

This recovery and redeposition approach has been shown to preserve particle size and mineralogical characteristics while improving particle dispersion and reducing agglomeration relative to direct-on-filter SEM analysis [21]. While the archived samples span a range of storage durations, no visible evidence of filter degradation or particle alteration was observed during SEM analysis. Nevertheless, it cannot be definitively confirmed that particle agglomeration or dispersion behavior was identical between earlier and later samples, and this represents a potential source of uncertainty.

2.3. Dust Characterization

SEM-EDX analysis was conducted on all available RCMD samples. Preparation of the PC filters for analysis by SEM-EDX consisted of cutting a 9 mm subsection of the filter using a stainless-steel trephine, and sputter coating by Au/Pd to render the sample conductive. The 9 mm subsection was generally cut off-center to avoid higher dust loading that can occur on the center of the 37 mm filter inside the 2-piece sampling cassettes. Analyses were performed using an FEI Quanta 600 FEG environmental SEM (Hillsboro, OR, USA) equipped with a backscatter electron detector and a Bruker Quantax 400 EDX system (Ewing, NJ, USA). Two computer-controlled routines—one targeting submicron particles and one targeting supramicron particles—were used to locate, size, and collect spectra for individual particles [22]. For each sample, the target count was approximately 300 particles in the submicron range and 500 particles in the supramicron range, consistent with prior RCMD particle studies [22]. Notably, while the SEM–EDX approach enables detailed characterization of particles down to about 100 nm, the present analysis was limited to particles with projected area diameters $\geq$300 nm. This threshold was applied to minimize uncertainties associated with automated EDX analysis of smaller particles, for which X-ray signal intensity and compositional reliability can be limited. As a result, particles in "nanoscale" range (i.e., typically defined as <100 nm) are not fully represented in the present dataset.

Prior to full analysis, each mounted sample was inspected to verify that particle loading density (PLD) fell within an empirically determined optimal range (approximately 0.001–0.035 particles per μm^2 in the supramicron range), which allows efficient particle detection while minimizing spectral interference from neighboring particles [21]. If PLD was outside this range, the sample was re-prepared and reassessed.

From the full SEM-EDX analysis, elemental spectra from each particle were used to assign it to a predefined mineralogy class (C = carbonaceous, SIL = silicates, S = silica, HM = heavy minerals, CB = carbonates, O = other) following the general classification

criteria [22]. Estimated particle mass was calculated using class-specific density and shape-factor assumptions from previous work and particle mass was estimated from equivalent circular diameter assuming spheroidal geometry and mineral-specific densities.

Per Sarver et al. (2022), there are multiple silicate subclasses and a mixed-carbonaceous class [20]. For the present analysis, the silicate subclasses were consolidated into SIL to facilitate temporal comparison. Mixed carbonaceous particles were also combined with SIL because, particularly after sonication-based recovery and redeposition, they are likely to represent thin silicate particles whose spectra are influenced by the PC substrate [21,22]. Mass was not estimated for O particles since reliable density and shape assumption cannot be made.

2.4. Data Analysis

Particle-level data obtained from SEM-EDX analysis were aggregated on a per-sample basis to generate number-based and estimated mass-based mineralogy distributions, as well as particle size distributions for each mineralogy class and for all particles combined, following the approach established by Sarver et al. (2021) [22]. Particle counts from the submicron and supramicron SEM routines were merged to construct full size distributions. Because different total surface areas were analyzed in each routine, particle counts within each size range were normalized by the corresponding analyzed area prior to merging, yielding area-normalized particle number densities.

For evaluation of temporal trends, analyses were restricted to samples from the four regions represented in both the earlier and later sample sets (CA, NA, MW, and W), comprising 37 earlier and 30 later samples (Table 1). Differences between timeframes were assessed for number- and estimated mass-based mineralogy distributions and for D50 values for individual classes and for all particles combined.

For evaluation of temporal differences, analyses were restricted to samples from the four geographic regions represented in both the earlier and later datasets (i.e., central Appalachia, northern Appalachia, the Midwest, and the western United States), comprising 37 earlier samples and 30 later samples (Table 1). Differences between timeframes were assessed for number- and estimated mass-based mineralogy distributions, as well as for median particle diameter (D50) values for individual mineralogy classes and for all particles combined. Statistical comparisons between earlier and later samples were conducted using two-sample *t*-tests assuming unequal variance ($\alpha = 0.05$). These tests were used to evaluate overall differences between timeframes without explicitly accounting for geographic region.

Notably, because mineralogy results are expressed as compositional data (i.e., fractions summing to 100%), and given the relatively small and uneven sample sizes across regions, statistical comparisons are interpreted cautiously. In particular, results are used to support observed patterns in the data rather than to establish definitive differences between timeframes. Emphasis is placed on consistent directional trends across regions and between number- and mass-based metrics, rather than on individual *p*-values.

Samples from the CKY and AL regions were excluded from all statistical comparisons due to the absence of corresponding later samples. Results from those regions are presented descriptively to provide contextual comparison with other regions in the earlier dataset.

3. Results and Discussion

A complete dataset for all individual samples analyzed in this study is provided in the Supplementary Materials. For each sample, the table includes the number of particles analyzed in the submicron and supramicron SEM routines, number-based and estimated mass-based mineralogy distributions, and median particle diameters (D50) for each miner-

alogy class as well as for all particles combined. These data form the basis for the regional and temporal summaries presented below.

Representative SEM images of redeposited respirable coal mine dust (RCMD) particles are also included in the Supplementary Materials. These images are provided to illustrate the heterogeneous nature of RCMD and the particle morphologies commonly observed in this study; however, they are not used directly in the quantitative analyses reported here.

3.1. Mineralogy Composition of RCMD

For context, the mineralogy classes used in this study can be broadly associated with different particulate sources in underground coal mines. C particles originate primarily from the coal seam and, at very fine sizes, may also include contributions from diesel engine emissions [2,23]. SIL and S particles are largely associated with disturbance of adjacent rock strata during cutting or drilling activities, while HM particles represent less abundant but compositionally distinct mineral phases [22]. CB particles are most commonly associated with rock-dusting materials applied to mitigate explosion hazards, although in some regions—particularly parts of the MW—carbonate-bearing strata may also contribute CB particles (Jaramillo et al., 2022) [13]. These associations are not exclusive but provide a useful framework for interpreting regional and temporal differences in RCMD composition.

Figure 1 summarizes RCMD mineralogy distributions by geographic region and timeframe, including all mineralogy classes. In the number-based results (Figure 1, left), RCMD across most regions is dominated by C and SIL particles, with S, CB, HM, and O comprising smaller fractions. However, the relative proportions of these dominant classes vary substantially by region, reflecting differences in geology, mining practices, and dust-control strategies [2,12,13,20,22,24].

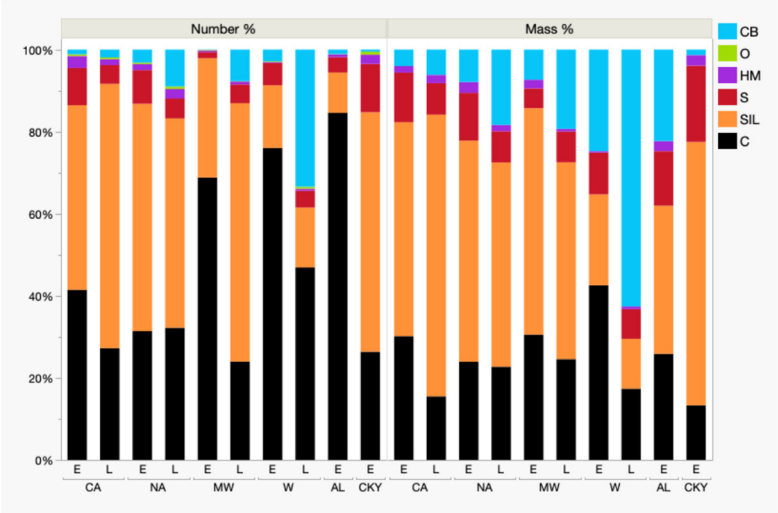


Figure 1. Mineralogy distributions for respirable coal mine dust (RCMD) by geographic region (CA, NA, MW, W, AL, and CKY) and time frame (E = 2003–2005, or L = 2018–2020). Results include all samples shown in Table 1 and are presented as mean number percentages (**left**) and mean estimated mass percentages (**right**). Mineralogy classes include C, SIL, S, HM, CB, and O. To facilitate temporal comparisons, only data from the CA, NA, MW, and W regions were included in statistical analyses; data from AL and CKY are shown for descriptive context only.

In the CA and NA regions, where paired earlier and later samples are available, RCMD exhibits consistently high SIL fractions by number, indicating a strong influence of rock strata-derived dust across both timeframes. In CA, later samples show a clear increase in SIL and a decrease in both C and S, indicating a growing relative contribution of non-quartz silicate material within the rock-strata derived fraction. In NA, C remains relatively

stable, while the rock-strata derived fraction shifts from S toward SIL, again indicating a compositional change within rock strata-derived dust rather than a major change in coal-to-rock ratios. Samples from CKY, available only for the earlier timeframe, exhibit mineralogy distributions similar to those observed in CA and NA, with relatively high SIL fractions and lower C, and notably the highest mean S fraction among the regions represented in the earlier dataset.

In contrast, samples from the W region—and from the MW region in the earlier timeframe—exhibit substantially higher C fractions by number and correspondingly lower SIL fractions. These high C fractions appear to be related, at least in part, to diesel particulates, some of which could be visually identified in SEM images (e.g., see Supplementary Materials). Samples from AL (available only for the earlier timeframe) show mineralogy distributions more similar to those observed in W and earlier MW samples.

The mass-based results (Figure 1, right) show systematic shifts relative to the number-based distributions. Across all regions, the fraction of C decreases on a mass basis, whereas the fraction of CB increases, reflecting class-specific differences in particle size and density (C being finer and less dense, and CB being coarser and more dense. This number-to-mass reduction in C is most pronounced in the W and AL regions and in the earlier MW samples, which corroborates the apparent influence of very fine diesel particulates in the particle counts. In W and AL, the reduction the C fraction moving from number to mass data is largely offset by an increase in CB, whereas in earlier MW samples it is not; the trend in the MW data is consistent with a greater contribution of particles from carbonate-bearing rock strata rather than applied rock dust products in that region [13].

Notably, across all four regions with paired datasets (CA, NA, MW, and W), Figure 1 shows a consistent increase in the CB fraction from the earlier to the later samples, regardless of whether results are presented on a number- or mass-based basis. This pattern is consistent with increased rock dusting intensity following the Sago (2006) and Upper Big Branch (2010) mine disasters and the subsequent strengthening of explosion-control requirements [2,3,16].

Results of the statistical comparisons for mineralogy distributions are presented in Table 2 and support the general trends observed in Figures 1 and 2, including decreases in C and S fractions and increases in SIL and CB fractions in later samples. However, these differences were not consistent across regions, indicating that regional variability may contribute to the observed temporal patterns.

Table 2. Results of statistical comparisons between earlier (2003–2005) and later (2018–2020) samples for number-based and estimated mass-based mineralogy distributions across the four regions with paired datasets (CA, NA, MW, and W). Mass-based analyses exclude the "other" (O) class because particle mass could not be estimated for that category. *p*-values below α (0.05) are shown in red. Statistical results are presented to support observed trends and should be interpreted cautiously given the compositional nature of the data and uneven sample representation across regions.

	C	SIL	S	HM	CB	O
number %	0.0009	0.0069	0.0432	0.9248	0.0372	0.2285
estimated mass %	0.0068	0.1505	0.0694	0.6541	0.1864	-

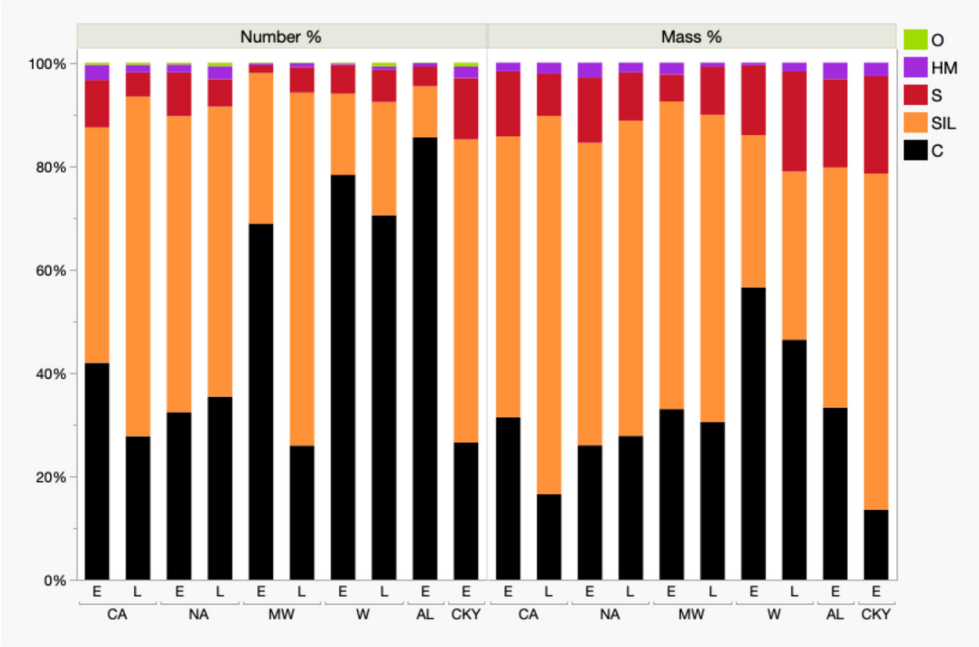


Figure 2. Mineralogy distributions for respirable coal mine dust (RCMD) by geographic region (CA, NA, MW, W, AL, and CKY) and time frame ((E = 2003–2005, or L = 2018–2020), excluding carbonate particles (CB). Results include all samples shown in Table 1 and are presented as mean number percentages (**left**) and mean estimated mass percentages (**right**), with remaining mineralogy classes renormalized to 100%. Mineralogy classes include C, SIL, S, HM, and O. To facilitate temporal comparisons, only data from the CA, NA, MW, and W regions were included in statistical analyses; data from AL and CKY are shown for descriptive context only.

As noted above, CB particles are most commonly associated with rock-dusting products applied to mitigate explosion hazards [2,12,13,16]. The inclusion of CB can therefore obscure trends related more directly to dust derived from mine geology (i.e., coal seams and adjacent rock strata). To better isolate compositional differences associated with mining and drilling activities, Figure 2 presents mineralogy distributions with CB excluded and the remaining classes renormalized to 100%.

Overall, Figure 2 confirms the major trends observed in Figure 1, particularly the increase in rock-strata derived material and the redistribution between S and SIL over time. In the number-based results excluding CB (Figure 2, left), the shift from S to SIL in both CA and NA becomes more apparent. In CA, the decrease in C relative to total mineral particles (SIL + S + HM) is now clearly evident, indicating a growing influence of rock-strata derived dust in later samples. In NA, C remains relatively stable while the rock-strata derived fraction shifts from S toward SIL, consistent with changes in the composition of dust being generated the rock strata rather than changes in overall coal-to-rock ratios.

In addition to excluding CB, the mass-based results in Figure 2 (right) minimize the influence of very fine C particles. Comparing trends between the number- and mass-based results again highlights the contribution of diesel particulates to samples from the W and AL regions, and the earlier samples from the MW region. In the W region, the mass-based results indicate a slight increase in the rock-strata derived dust relative to coal-derived dust.

3.2. RCMD Particle Size

Figure 3 summarizes the distributions of median particle diameters (D50 values) by geographic region and timeframe (Earlier period denoted as E and later period denoted as L). Results are shown separately for individual mineralogy classes (colored box-and-whisker plots), and for each class the corresponding distribution for all particles combined

(gray box-and-whisker plots) is shown to provide context for how that class contributes to the overall particle size distribution.

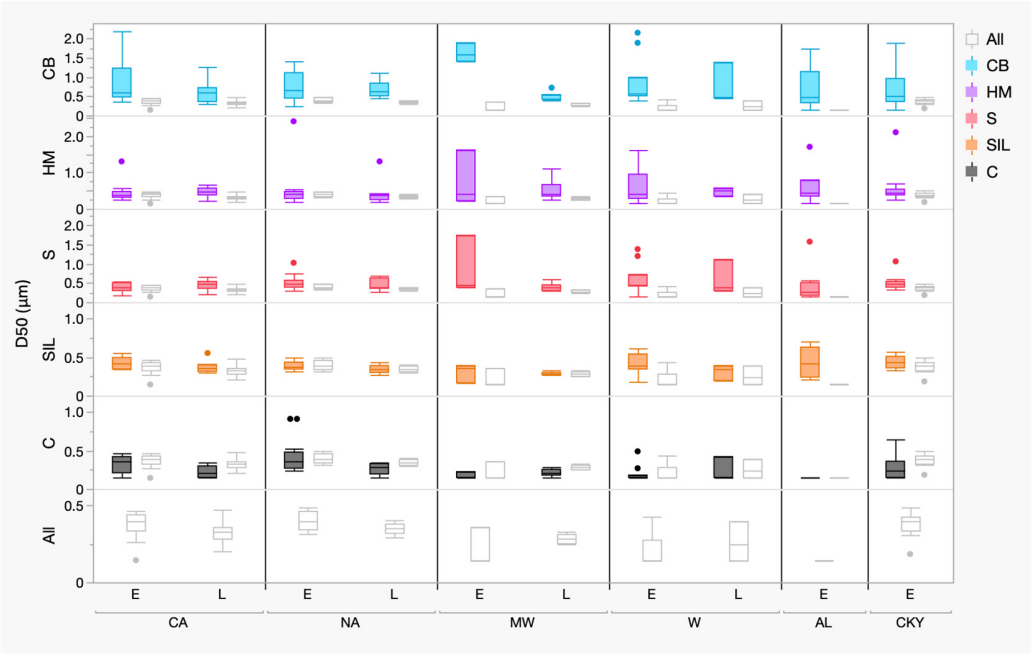


Figure 3. Distributions of median particle diameters (D50) for respirable coal mine dust (RCMD) particles by geographic region and timeframe (E = 2003–2005, or L = 2018–2020). Results include all samples shown in Table 1 and are presented for individual mineralogy classes (colored box-and-whisker plots), with corresponding distributions for all particles combined shown in gray for context. Boxes represent the interquartile range with median values indicated; whiskers extend to 1.5× the interquartile range, and points denote outliers. Mineralogy classes include C, SIL, S, HM, and CB.

Across all regions and timeframes, systematic differences in particle size are evident among mineralogy classes. C particles consistently exhibit the smallest median diameters, a pattern that likely reflects the influence of very fine particles, including diesel particulates, within this class [17,23]. In contrast, CB and HM particles tend to be substantially coarser, while SIL and S particles generally fall between these extremes. These class-specific size differences are consistent with prior observations for a larger set of RCMD samples collected in the later timeframe reported by Sarver et al. (2021) [22] and help explain some of the contrasting behavior observed between number-based and mass-based mineralogy distributions discussed in Section 3.1.

When all particles are considered together (gray plots in Figure 3), the D50 values are strongly influenced by the most numerous fine particles, particularly those in the C class. As a result, the "all particles" size distributions tend to closely track the behavior of carbonaceous particles in most regions. In contrast, the colored box-and-whisker plots highlight how less numerous but coarser particle classes—such as CB and HM—can exert a disproportionate influence on mass-based metrics despite contributing relatively few particles by number [2].

In the CA region, later samples show a clear decrease in the overall ("All") D50, driven primarily by decreases in both C and SIL median sizes, while S, HM, and CB exhibit relatively stable or slightly higher D50 values. This pattern indicates that RCMD in later CA samples contains a larger fraction of very fine particles overall, even as some coarser mineral particles remain present. Notably, Section 3.1 showed that both number- and mass-based mineralogy results in CA indicate a greater influence of rock-strata derived particles (particularly SIL) in later samples. The apparent contradiction between finer SIL medians

and higher SIL mass fractions can be explained by the strongly nonlinear relationship between particle size and mass: because mass scales approximately with the cube of particle diameter, a relatively small population of coarse SIL particles can dominate the SIL mass even when the median SIL size shifts downward due to an increased abundance of fine particles. Figure 3 further shows that the reduction in D50 for C was greater than for SIL, indicating that the increase in very fine particles in CA was more strongly driven by carbonaceous material than by silicates. Taken together, these results are consistent with a broader and more heterogeneous SIL size distribution in later CA samples, rather than a simple shift toward uniformly coarser or finer silicate dust [2,25].

In the NA region, median particle sizes for most mineralogy classes change little between earlier and later samples, including for C, SIL, and S, and the overall ("All") D50 remains relatively stable. Consistent with this, Figures 1 and 2 show that both number- and mass-based mineralogy in NA exhibits only modest temporal changes, with a slight increase in C and a corresponding decrease in the relative contribution of rock-strata derived particles. Together, these results indicate that temporal changes in RCMD in this region are driven more by shifts in source contributions than by changes in particle size distributions.

In the MW region, particle size data show that earlier samples had much smaller C median diameters than later samples (Figure 3), consistent with the strong contrast between number- and mass-based C fractions observed in Figure 2. Later MW samples, by contrast, show slightly larger C median diameters and more similar C fractions on a number- and mass-basis, indicating a greater contribution from coarser carbonaceous material more consistent with coal dust. These differences between the earlier and later samples are consistent with reduced influence of very fine carbonaceous particles and may reflect changes in diesel equipment and emission controls over the period of study [2,3].

In the W region, few differences in particle size distributions for individual mineralogy classes can be observed between earlier and later samples in Figure 3. While substantial differences are evident in Figure 2 between number-based and mass-based metrics within each timeframe—reflecting the influence of fine C particles and coarse CB particles—the median sizes of individual classes do not exhibit strong temporal trends, indicating relative stability in dust-generation mechanisms and controls over the period of study.

Results of the statistical comparisons for particle size (D50) are presented in Table 3. These results are consistent with the trends observed in Figure 3, indicating differences between earlier and later samples for the C, SIL and CB classes. As discussed above, the magnitude and direction of these differences vary across regions.

Table 3. Results of statistical comparisons between earlier (2003–2005) and later (2018–2020) samples for median particle diameter (D50) by mineralogy class and for all particles combined across the four regions with paired datasets (CA, NA, MW, and W). *p*-values below α (0.05) are shown in red. Statistical results are presented to support observed trends and should be interpreted cautiously given sample size limitations and uneven sample representation across regions.

	C	SIL	S	HM	CB	Overall
D50	0.0220	0.0019	0.2631	0.4425	0.0184	0.8409

Interestingly, in prior work focused exclusively on RCMD samples from the later timeframe, S particles were generally found to be finer than SIL particles. In the present study, SIL particles often exhibit smaller D50 values than S across both timeframes. This difference likely reflects a combination of factors, including differences in regional representation, the inclusion of mixed-carbonaceous particles within the SIL class in the present analysis, and differences in sample preparation (direct-on-filter analysis in the prior work versus

recovery and redeposition here), all of which can influence particle dispersion and apparent size distributions [21].

It is also noted that the recovery and redeposition process may influence particle dispersion and agglomeration to some degree, particularly for archived samples of differing age, although no systematic artifacts were observed in the present analysis.

3.3. Synthesis of Temporal Trends and Implications for Mining Practices

Taken together, the results presented in Sections 3.1 and 3.2 indicate that changes in RCMD characteristics over the study period were generally subtle and region dependent. Most mineralogy classes did not exhibit a uniform temporal trend across all regions examined—on the basis of either RCMD composition or median particle size. Because these comparisons are based on samples collected from broadly comparable dust-generating environments rather than identical sampling locations, the results are best interpreted as reflecting general changes in dust characteristics rather than site-specific trends. Moreover, the study period corresponds to a time during which multiple aspects of underground coal mining evolved, including dust control practices (e.g., water sprays and ventilation), cutting methods, and equipment; however, specific operational changes likely varied at the individual mine level.

The primary exception to regional nuance was the observed consistent increase in CB particles in later samples across all regions with paired datasets. This pattern represents the most coherent temporal signal observed in the study and fits with expanded rock-dusting requirements implemented following the 2006 Sago and 2010 Upper Big Branch mine disasters [2,12,16]. The increase in CB particles observed across regions suggests that enhanced rock-dusting practices have influenced the respirable dust fraction in U.S. underground coal mines. While rock dust products are applied primarily to mine surfaces to mitigate explosion hazards, these results show that carbonate materials can contribute appreciably to RCMD composition—and, in some cases, to its mass concentration. The variability in CB abundance among regions and mines likely reflects differences in rock-dust application methods and intensity, mine layout and ventilation, and local geology, as well as the specific sampling locations represented in this dataset. Nevertheless, the consistent temporal increase across regions points to the broad impact of regulatory and operational changes during the period between the two sample sets. At the same time, it is important to note that carbonate particles are generally considered less hazardous to respiratory health than silica-bearing particles, acting primarily as irritants rather than fibrotic agents [26,27].

Interpretation of coal-derived contributions is complicated by the fact that the C class includes both coal dust and diesel particulates, particularly at very fine sizes [17,23]. For this reason, mass-based metrics—which are less influenced by very fine diesel particulates—provide a more reliable indicator of coal versus rock contributions. In CA, the mass-based results show a decrease in the C fraction together with a corresponding increase in SIL, indicating that RCMD became more influenced by rock-strata derived material over the period of study. Notably, however, the S fraction declined slightly over time, suggesting a shift within the rock-derived component toward a greater proportion of non-quartz silicate material. This pattern may reflect operational adjustments aimed at limiting silica generation in response to increased awareness of silica exposure risks [2,20,28], although regional differences in geology and mining conditions could also be a factor.

In contrast to CA, both number- and mass-based results in NA indicate a modest increase in the C fraction over time accompanied by relatively stable particle size distributions. This pattern suggests a reduced relative contribution from rock-strata derived dust in later samples, potentially reflecting different operational responses to silica exposure concerns

or differences in mining conditions relative to central Appalachia [20,29]. The consistency between number-based and mass-based metrics in NA further supports the interpretation that this shift reflects real changes in dust sources rather than size-driven artifacts.

Evidence for changes in diesel-related contributions to RCMD is limited, but the MW region results are consistent with a reduced influence of very fine carbonaceous particles in later samples—which broadly aligns with regulatory and technological efforts over the past two decades to reduce diesel emissions through improved engine standards and cleaner equipment [2,3]. Interpretation in other regions remains uncertain because the C class reflects multiple sources, including both coal dust and diesel particulates. It is also important to note that ultrafine particles, including diesel-derived nanoparticles, may contribute disproportionately to respiratory health risks due to their high number concentrations and surface area despite their limited contribution to mass [2,18]; however, such particles fall below the lower size threshold of the present analysis and are therefore not captured in this study. In the western region, RCMD composition and particle size characteristics were remarkably similar between the earlier and later samples, suggesting little change in dominant dust sources or controls over the study period. Across all regions, particle size results do not support a consistent shift toward finer respirable dust over the period examined, but instead indicate class-specific and regionally variable changes in particle size distributions.

Finally, this study demonstrates the value of particle-level characterization for understanding RCMD beyond conventional mass-based metrics. By combining mineralogical classification with particle size analysis, this approach provides a more detailed understanding of dust sources and their evolution over time. The use of archived samples further highlights the potential for retrospective analyses to evaluate long-term changes in mining environments and could support future efforts to link evolving dust characteristics with occupational health outcomes. However, it must be emphasized that the present study is not designed to directly assess health outcomes. Given the long latency associated with most dust-related occupational lung diseases [29], changes in RCMD composition or particle size during the period evaluated here are unlikely to be directly reflected in the current disease burden. Addressing such questions will require access to well-characterized archived RCMD samples from substantially earlier periods, along with comparable analytical methods.

4. Conclusions

Mining practices and operating conditions are continually evolving, and the respirable fraction of coal mine dust is accordingly expected to change in composition and particle characteristics over time. In this study, particle-level analyses were used to compare respirable coal mine dust (RCMD) samples collected during 2003–2005 and 2018–2020.

The most consistent temporal change observed was an increase in carbonate particles, on both a number and mass basis, across all regions with paired datasets. This finding is consistent with expanded rock-dusting practices and demonstrates that such practices have influenced the composition of respirable dust. Other changes in RCMD were more modest and region dependent. Shifts in the relative contributions of coal- and rock-strata–derived dust were observed over the study period; however, these shifts were not consistent across regions. Corresponding changes in mineralogy and particle size distributions were also region dependent. No consistent shift toward finer respirable dust was observed over the study period.

Interpretation of regional trends should be approached with caution due to limitations in sample availability and representativeness, particularly in the Midwest and Western regions where the number of samples was relatively small. In addition, differences in specific

sampling locations between the earlier and later datasets may contribute to variability in the observed results. The use of archived samples also introduces some uncertainty related to potential differences in sample handling and recovery, although no systematic artifacts were observed. These limitations should be considered when interpreting temporal changes in RCMD characteristics.

Nevertheless, this study demonstrates the value of particle-level characterization for evaluating RCMD beyond conventional mass-based metrics. The approach used here provides improved insight into dust composition and particle characteristics and highlights the potential for retrospective analyses of archived samples to assess changes in mining environments over time.

Supplementary Materials: The following supporting information can be downloaded at: https://www.mdpi.com/article/10.3390/mining6020027/s1, Table S1: Summary of SEM-EDX data for all samples. Timeframe: L = later, E = earlier; Geographic Region: NA = northern Appalachia, CA = central Appalachia, CKY = central Kentucky, MW = mid-west, W = west, AL = Alabama; Sampling Location: P = production, B = Roof bolter, F = feeder breaker, I = intake, R = return, AM = active mining; Mineralogy class: C = carbonaceous, SIL = silicates, S = silica, HM = heavy minerals, CB = carbonates, O = others; Figure S1: Representative SEM-EDX images of RCMD samples from each region and timeframe. For each secondary electron (SE), a paired elemental map is shown with aluminum (Al) and silicon (S) highlighted. Particles appearing bright green are interpreted as silica; particles appearing yellow or orange are interpreted as aluminum-bearing silicates (i.e., which are the predominant silicates in RCDM); particles appearing gray are most likely carbonaceous or carbonates. Images were captured at 5kV and 5000× magnification.

Author Contributions: Conceptualization, E.S.; methodology, E.S., Ç.K. and S.G.A.; field work, E.A.; formal analysis, Ç.K., S.G.A. and E.S.; data curation, Ç.K. and S.G.A.; writing—original draft preparation, Ç.K. and E.S.; writing—review and editing, E.A., Ç.K., S.G.A. and E.S.; supervision, E.S.; project administration, E.S.; funding acquisition, E.S. All authors have read and agreed to the published version of the manuscript.

Funding: This work was funded by the Alpha Foundation for the Improvement of Mine Safety and Health (Grant: AFCTG20-104).

Data Availability Statement: The data presented in this study are available in the Supplementary Information or upon reasonable request from the corresponding author.

Acknowledgments: We gratefully acknowledge the CDC/NIOSH Pittsburgh Mining Research Division for provision of the archived dust samples, especially George Luxbacher, Jay Colinet and Milan Yekich. We also appreciate the many mine partners who provided mine access and logistical support for collection of the more recent dust samples investigated here.

Conflicts of Interest: The authors declare no conflicts of interest.

References

1. Doney, B.; Blackley, D.; Hale, J.; Halldin, C.; Kurth, L.; Syamlal, G.; Laney, A.S. Respirable coal mine dust in underground mines, United States, 1982–2017. *Am. J. Ind. Med.* **2019**, *62*, 478–485. [CrossRef] [PubMed]
2. National Academies of Sciences, Engineering, and Medicine (NASEM). *Monitoring and Sampling Approaches to Assess Underground Coal Mine Dust Exposures*; The National Academies Press: Washington, DC, USA, 2018.
3. MSHA. *Lowering Miners' Exposure to Respirable Coal Mine Dust, Including Continuous Personal Dust Monitors*; Federal Register: Washington, DC, USA, 2017.
4. Agioutanti, E.; Keles, C.; Sarver, E. A thermogravimetric analysis application to determine coal, carbonate, and non-carbonate minerals mass fractions in respirable mine dust. *J. Occup. Environ. Hyg.* **2020**, *17*, 47–58. [CrossRef]
5. Antao, V.C.; Petsonk, E.L.; Sokolow, L.Z.; Wolfe, A.L.; Pinheiro, G.A.; Hale, J.M.; Attfield, M.D. Rapidly progressive coal workers' pneumoconiosis in the United States: Geographic clustering and other factors. *Int. J. Occup. Environ. Med.* **2005**, *62*, 670–674. [CrossRef]

6. Laney, A.S.; Attfield, M.D. Coal workers' pneumoconiosis and progressive massive fibrosis are increasingly more prevalent among workers in small underground coal mines in the United States. *Occup. Environ. Med.* **2010**, *67*, 428–431. [CrossRef]
7. Suarthana, E.; Laney, A.S.; Storey, E.; Hale, J.M.; Attfield, M.D. Coal workers' pneumoconiosis in the United States: Regional differences 40 years after implementation of the 1969 Federal Coal Mine Health and Safety Act. *Int. J. Occup. Environ. Med.* **2011**, *68*, 908–913. [CrossRef]
8. Blackley, D.J.; Crum, J.B.; Halldin, C.N.; Storey, E.; Laney, A.S. Resurgence of progressive massive fibrosis in coal miners—Eastern Kentucky. *MMWR Morb. Mortal. Wkly. Rep.* **2016**, *65*, 1385–1389. [CrossRef]
9. Blackley, D.J.; Reynolds, L.E.; Short, C.; Carson, R.; Storey, E.; Halldin, C.N.; Laney, A.S. Progressive massive fibrosis in coal miners from 3 clinics in Virginia. *J. Am. Med. Assoc.* **2018**, *319*, 500–501. [CrossRef]
10. Almberg, K.; Halldin, C.; Friedman, L.; Go, L.H.T.; Rose, C.; Hall, N.; Cohen, R. Increased odds of mortality from non-malignant respiratory disease and lung cancer are highest among US coal miners born after 1939. *Occup. Environ. Med.* **2023**, *80*, 121–128. [CrossRef]
11. Harris, D.; Almberg, K.; Blackley, D.; Cohen, R.; Edwards, C.; Johnson, B.; Hall, N.B. Progressive Massive Fibrosis Identified at Federally Funded Black Lung Clinics in the US. *JAMA* **2024**, *331*, 438–440. [CrossRef] [PubMed]
12. Pokhrel, N.; Keles, C.; Jaramillo, L.; Agioutanti, E.; Sarver, E. Direct-on-Filter FTIR Spectroscopy to Estimate Calcite as a Proxy for Limestone 'Rock Dust' in Respirable Coal Mine Dust Samples. *Minerals* **2021**, *11*, 922. [CrossRef]
13. Jaramillo, L.; Agioutanti, E.; Keles, C.; Sarver, E. Thermogravimetric Analysis of Respirable Coal Mine Dust for Source Apportionment. *J. Environ. Occup. Health* **2022**, *19*, 568–579. [CrossRef]
14. Blackley, D.J.; Halldin, C.; Wang, M.; Laney, A.S. Small mine size is associated with lung function abnormality and pneumoconiosis among underground coal miners in Kentucky, Virginia and West Virginia. *Occup. Environ. Med.* **2014**, *71*, 690–694. [CrossRef]
15. MSHA. *Lowering Miners' Exposure to Respirable Crystalline Silica and Improving Respiratory Protection*; Federal Register: Washington, DC, USA, 2023.
16. Luo, Y.; Wang, D.; Cheng, J. Effects of rock dusting in preventing and reducing intensity of coal mine explosions. *Int. J. Coal Sci. Technol.* **2017**, *4*, 102–109. [CrossRef]
17. Birch, M.E.; Noll, J.D. Submicrometer elemental carbon particles in coal mine dust. *Ann. Occup. Hyg.* **2004**, *48*, 163–176.
18. Fan, L.; Liu, S. Respirable nano-particulate generations and their pathogenesis in mining workplaces: A review. *Int. J. Coal Sci. Technol.* **2021**, *8*, 179–198. [CrossRef]
19. Pan, L.; Golden, S.; Assemi, S.; Sime, M.F.; Wang, X.; Gao, Y.; Miller, J. Characterization of particle size and composition of respirable coal mine dust. *Minerals* **2021**, *11*, 276. [CrossRef]
20. Keles, C.; Pokhrel, N.; Sarver, E. A study of respirable silica in underground coal mines: Sources. *Minerals* **2022**, *12*, 1115. [CrossRef]
21. Greth, K.M.; Afrouz, S.G.; Sarver, E.A.; Keles, C. A sample recovery and redeposition method for SEM-EDX analysis of respirable coal mine dust collected on PVC filters. *Min. Metall. Explor.* **2024**, *41*, 1145–1163.
22. Sarver, E.; Kele¸s, Ç.; Afrouz, S.G. Particle size and mineralogy distributions in respirable dust samples from 25 US underground coal mines. *Int. J. Coal Geol.* **2021**, *247*, 103851. [CrossRef]
23. Eskanlou, A.; Arnold, B.J. Toxicity of respirable coal dust: An overview of origin, chemistry, mechanisms, and possible remedies. *Int. J. Coal Sci. Technol.* **2026**, *13*, 1. [CrossRef]
24. Wang, X.; Abbasi, B.; Elahifard, M.; Osho, B.; Chen, L.-W.A.; Chow, J.C.; Watson, J.G. Coal Mine Dust Size Distributions, Chemical Compositions, and Source Apportionment. *Minerals* **2024**, *14*, 1122. [CrossRef]
25. Volkwein, J.C.; Vinson, R.P.; Page, S.J.; McWilliams, L.J.; Joy, G.J.; Mischler, S.E.; Tuchman, D.P. *Laboratory and Field Evaluation of Dust Control Technologies*; NIOSH Report 2006, DHHS (NIOSH) 2006-142; Centers for Disease Control and Prevention: Atlanta, Georgia, 2006.
26. Jelić, T.M.; Estalilla, O.C.; Sawyer-Kaplan, P.R.; Plata, M.J.; Powers, J.T.; Emmett, M.; Kuenstner, J.T. Coal mine dust desquamative chronic interstitial pneumonia: A precursor of dust-related diffuse fibrosis and of emphysema. *Int. J. Occup. Environ. Med.* **2017**, *8*, 153–165. [CrossRef] [PubMed]
27. Khaliullin, T.O.; Kisin, E.R.; Yanamala, N.; Guppi, S.; Harper, M.; Lee, T.; Shvedova, A.A. Comparative pulmonary toxicity of respirable carbonate versus quartz particles. *Toxicol. Appl. Pharmaco.* **2019**, *362*, 67–76. [CrossRef] [PubMed]
28. Shao, Y.; Almberg, K.S.; Friedman, L.S.; Cohen, R.A.; Go, L.H.T. Thin seams and small mines are associated with higher exposures to respirable crystalline silica in US underground coal mines. *Int. J. Occup. Environ. Med.* **2024**, *81*, 308–312. [CrossRef] [PubMed]
29. Cohen, R.A.; Petsonk, E.L.; Rose, C. Coal mine dust lung disease: New lessons from old exposure. *Am. J. Respir. Crit. Care Med.* **2016**, *193*, 1178–1185.

Disclaimer/Publisher's Note: The statements, opinions and data contained in all publications are solely those of the individual author(s) and contributor(s) and not of MDPI and/or the editor(s). MDPI and/or the editor(s) disclaim responsibility for any injury to people or property resulting from any ideas, methods, instructions or products referred to in the content.